

0017-9310(95)00197-2

# Free convective mass transfer at down-pointing pyramidal electrodes

J. KRYSA

Department of Inorganic Technology, Institute of Chemical Technology, 16628 Prague 6, The Czech Republic

and

A. A. WRAGG†

School of Engineering, Exeter University, North Park Road, Exeter EX4 4QF, U.K.

(Received 9 June 1994 and in final form 17 March 1995)

**Abstract**—A limiting current technique was used for the measurement of the free convective mass transfer rate at entire down-pointing pyramids and also at the individual faces of the pyramids. The cathodic deposition of  $\text{Cu}^{2+}$  ions at electrodes of varying geometries was used as the mass transfer process, the supporting electrolyte being sulphuric acid. The mass transfer rate at a single inclined pyramidal surface was correlated by the equation

$$Sh_{L,\theta} = 0.78(Ra_{L,\theta})^{0.25}$$

for the  $Ra_{L,\theta}$  range  $9.3 \times 10^6$  to  $2 \times 10^{11}$ . The mass transfer data for the entire pyramid were correlated using a method which includes an interference factor taking account of the fact that the upward-facing horizontal surface is exposed to fluid which has already been depleted in copper ions. The dependence of the interference factor on the aspect ratio of the pyramid ( $L/b$ ) was established.

## 1. INTRODUCTION

This paper describes an experimental investigation of mass transfer in free convection at down-pointing pyramidal electrodes using the well-known limiting diffusion current technique (LDCT) of mass transfer measurement. The down-pointing pyramidal electrode is a case of a three-dimensional object with one upward facing horizontal triangular face and three inclined triangular faces.

Several previous accounts of work on free convective mass transfer at inclined surfaces [1–3], upward horizontal surfaces [4–7] and three-dimensional objects [8–11] are known to the authors, all of which made use of the LDCT. Patrick *et al.* [1], as part of a broader investigation, studied free convection mass transfer to inclined down-facing rectangular surfaces and the results were well correlated by the equation

$$Sh_{L,\theta} = 0.68(Ra_L \cos \theta)^{0.25} \quad (1)$$

for  $6 \times 10^4 \leq Ra_{L,\theta} \leq 3 \times 10^9$ ,  $\theta$  being the inclination angle from vertical. The results of Fouad and Ahmed [3] for down-facing planes also follow equation (1), even up to a  $Ra_{L,\theta}$  value of  $10^{12}$ , suggesting, rather surprisingly, that a predominantly laminar flow persists up to this high value of Rayleigh number.

Free convective mass transfer at horizontal electrodes has also received considerable attention using the electrochemical method [4–6], diameter (for circular planes) [5, 6] or length (for rectangles) [4] being used as characteristic dimensions in correlating equations. Lloyd and Moran [7] investigated natural convection adjacent to unshrouded upward facing horizontal surfaces formed by circular, square, rectangular and right triangular planforms. The data for all planforms were reduced to a single correlation using the characteristic length recommended by Goldstein *et al.* [12]

$$L_G = \frac{\text{surface area}}{\text{surface perimeter}} \quad (2)$$

The data for the turbulent regime were correlated by the expression

$$Sh = 0.15(Ra)^{0.33} \quad (3)$$

in the range  $8 \times 10^6 \leq Ra \leq 1.6 \times 10^9$ . This characteristic length of equation (2) appears to bring all the data into the common correlation, including those for surfaces such as the right triangles.

Weber *et al.* [8] measured and correlated natural convection mass transfer from a variety of spherical and non-spherical three-dimensional objects, including pyramids in several orientations. The charac-

† Author to whom correspondence should be addressed.



copper. Each electrode was supported using a 1 mm diameter steel wire glued into a hole in the centre of the horizontal base. This wire also served as a current carrier. The wire was lacquered to insulate it from the electrolyte. The pyramidal cathodes were placed in the centre of the container. The counter electrode (anode) was a cylindrical copper mesh of diameter 14 cm and height 24 cm. The arrangement of the apparatus is similar to that shown previously [11]. The actual  $\text{Cu}^{2+}$  concentration was periodically determined by spectrophotometric analysis, to an accuracy of approximately 2%.

The usual electrical circuit for limiting current measurement was employed, consisting of a d.c. power supply with a voltage regulator, a high impedance voltmeter and a multi-range ammeter. Limiting currents were obtained by the well known procedure which has been reported in detail previously [14]. The anode acted as a reference electrode in view of its high area compared to that of the cathode. Under such conditions polarization is negligible at the anode and the cell current-voltage relationship depends only on the conditions prevailing at the cathode. The onset of the limiting current was sharp and reproducible, and its value was determined to an accuracy of  $\pm 2\%$ .

Table 1 lists all the geometric characteristics of the pyramids used. This work considers sets of pyramids with constant inclination angle  $\theta$ , constant length of inclined surface  $L$  and varying aspect ratios (length to side of base). In this investigation  $L$  ranged from 0.57 up to 7.86 cm and inclination angle from  $-4.5$  up to  $-50.8^\circ$ . Values of  $L$  are estimated to be accurate within 1–2%. Inclination angles are counted negative to indicate the down-facing orientation of the triangular pyramid faces and for consistency with the work described in [1].

The mass transfer controlled limiting currents at the inclined surface and at the upward facing horizontal surface were measured separately and in combination e.g. at the pyramid with three active inclined surfaces and at the entire pyramid with the upfacing top sur-

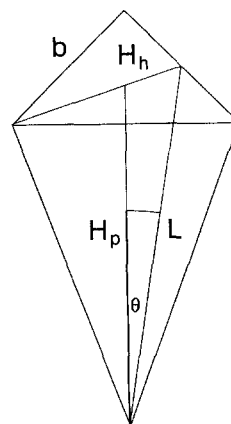


Fig. 1. Geometric parameters of down-pointing pyramids.

face also simultaneously active. Surfaces not required to be active were stopped off with lacquer.

The geometric parameters of the down pointing pyramids are illustrated in Fig. 1.

### 3. RESULTS AND DISCUSSION

#### 3.1. Mass transfer data calculations

For each experiment the mass transfer coefficient was calculated from the measured limiting current using the equation:

$$k = \frac{I_L}{AnFc_b} \quad (7)$$

The area in this equation was the total available for mass transfer for the particular experiment. The correction for the attachment of the supporting wire was small, never being more than 1.5% of the exposed area and usually being much less.

For the inclined triangular surfaces, the data were expressed in the form of a slant height Sherwood number and a slant height Rayleigh number

Table 1. Electrode geometries

| Pyramid | $b$<br>(cm) | $L$<br>(cm) | $\theta$<br>( $^\circ$ ) | $H_p$<br>(cm) | $H_h$<br>(cm) | $A_i$<br>( $\text{cm}^2$ ) | $A_{it}$<br>( $\text{cm}^2$ ) | $A_{pt}$<br>( $\text{cm}^2$ ) | $A_{it}/A_h$ | $L/b$ | $L_w$<br>(cm) | $\psi$ |
|---------|-------------|-------------|--------------------------|---------------|---------------|----------------------------|-------------------------------|-------------------------------|--------------|-------|---------------|--------|
| 1       | 1.05        | 0.57        | -31.5                    | 0.49          | 0.83          | 0.30                       | 0.90                          | 1.33                          | 2.06         | 0.54  | 0.42          | 0.62   |
| 2       | 2.15        | 1.19        | -31.5                    | 1.02          | 1.86          | 1.28                       | 3.87                          | 5.87                          | 1.93         | 0.55  | 0.91          | 0.64   |
| 3       | 3.60        | 1.97        | -31.5                    | 1.68          | 3.12          | 3.55                       | 10.64                         | 16.26                         | 1.89         | 0.55  | 1.50          | 0.64   |
| 4       | 5.34        | 2.96        | -31.5                    | 2.52          | 4.62          | 7.90                       | 23.71                         | 36.04                         | 1.92         | 0.55  | 2.25          | 0.64   |
| 5       | 7.14        | 3.95        | -31.5                    | 3.37          | 6.18          | 14.10                      | 42.31                         | 64.37                         | 1.92         | 0.55  | 3.00          | 0.64   |
| 6       | 1.16        | 1.96        | -10                      | 1.93          | 1.00          | 1.14                       | 3.41                          | 4.02                          | 5.81         | 1.69  | 1.15          | 0.62   |
| 7       | 2.31        | 1.97        | -20                      | 1.85          | 2.00          | 2.28                       | 6.83                          | 9.14                          | 2.95         | 0.85  | 1.32          | 0.67   |
| 8       | 3.39        | 1.96        | -30                      | 1.70          | 2.94          | 3.22                       | 10.00                         | 14.98                         | 2.00         | 0.59  | 1.47          | 0.64   |
| 9       | 4.34        | 1.98        | -40                      | 1.52          | 3.76          | 4.30                       | 12.90                         | 21.05                         | 1.58         | 0.46  | 1.62          | 0.59   |
| 10      | 5.22        | 1.99        | -50                      | 1.28          | 4.52          | 5.20                       | 15.58                         | 27.38                         | 1.32         | 0.38  | 1.75          | 0.51   |
| 11      | 2.17        | 0.805       | -50.8                    | 0.51          | 1.88          | 0.87                       | 2.62                          | 4.66                          | 1.28         | 0.37  | 0.71          | 0.51   |
| 12      | 2.22        | 1.20        | -32.2                    | 1.06          | 1.92          | 1.33                       | 3.99                          | 6.12                          | 1.87         | 0.54  | 0.92          | 0.64   |
| 13      | 2.20        | 2.06        | -17.9                    | 2.00          | 1.91          | 2.27                       | 6.81                          | 8.91                          | 3.24         | 0.94  | 1.35          | 0.68   |
| 14      | 2.17        | 3.97        | -9.0                     | 3.93          | 1.88          | 4.31                       | 12.93                         | 15.03                         | 6.16         | 1.83  | 2.31          | 0.62   |
| 15      | 2.13        | 7.86        | -4.5                     | 7.83          | 1.84          | 8.37                       | 25.11                         | 27.07                         | 12.8         | 3.70  | 4.24          | 0.53   |

$$Sh_L = \frac{kL}{D} \quad (8)$$

$$Ra_{L,\theta} = \frac{g\Delta\rho L^3}{\mu D} \cos\theta. \quad (9)$$

This approach to data treatment was previously used for the correlation of free convective heat and mass transfer at inclined plates [1, 2, 20] and at cones with an insulated base [15].

The diffusivity of the  $Cu^{2+}$  ions was calculated using the equation

$$\frac{D\mu}{T} = (2.495 + 0.0173c_{CuSO_4} + 0.0692c_{H_2SO_4}) \times 10^{-15} \frac{N}{K} \quad (10)$$

due to Fenech and Tobias [4], where  $C$  is in  $\text{mol dm}^{-3}$ . Density and viscosity were calculated using data of Eisenberg *et al.* [16]. The  $\Delta\rho$  terms were taken from Wilke *et al.* [17]. The effect of migration on the copper deposition rate was negligible; the migration contribution for the highest concentration of copper sulphate (0.23 M) was 1.5% [18]. Values of  $Sh_0$  were calculated by the method outlined by Clift *et al.* [19].

### 3.2. Single active surfaces

Mass transfer coefficients for a single inclined triangular surface for different pyramid lengths for pyramids numbered 11–15 are shown in Fig. 2. These are dependent both on the length and inclination angle [1]. Due to this fact the effect of pyramid length and inclination angle were investigated separately. The mass transfer coefficients to a single inclined surface were measured at pyramids 1–5 (constant inclination

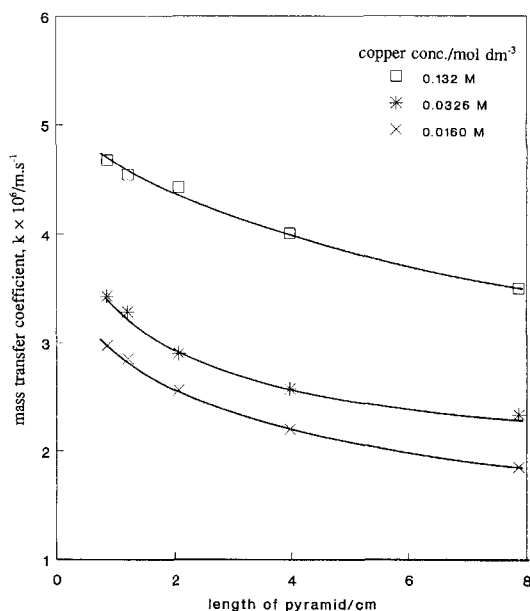


Fig. 2. The effect of length (and inclination angle) on mass transfer coefficient for a single face of down-pointing constant base pyramids for varying  $CuSO_4$  concentrations (pyramids 11–15).

angle, varying length (Fig. 3a)) and at pyramids 6–10 (constant length, varying inclination angle (Fig. 3b)). From Fig. 3a,b it follows that the mass transfer coefficient depends chiefly on the surface length and the inclination angle begins to show a greater influence for inclination angles greater than  $-40^\circ$ . The effect of both length and inclination angle for a single concentration of copper sulphate is shown in Fig. 3c. Values of  $K$  were plotted against  $L$  for pyramids 11–15 (curve c).  $K$  values on curve b were obtained as follows. To the lengths of pyramids 11–15 values of inclination angle were attributed according to Table 1. For each inclination angle (with the exception of  $-4.5^\circ$ ) values of  $K$  were taken from Fig. 3b.

A plot of  $Sh_L$  against  $Ra_{L,\theta}$  for the single inclined triangular surfaces is shown as Fig. 4. A least squares fit of the data yields the relation

$$Sh_L = 0.68(Ra_{L,\theta})^{0.259}. \quad (11)$$

Forcing a slope of 1/4, as has been reported in the literature for laminar flow on inclined planes [1, 2, 15, 20], gives

$$Sh_L = 0.78(Ra_{L,\theta})^{0.25} \quad (12)$$

for data in the  $Ra_{L,\theta}$  range  $9.3 \times 10^6$  to  $2 \times 10^{11}$ . This equation is plotted as the line in Fig. 4 and can be seen to represent the data well. The higher value of the coefficient in equation (12) for a single inclined triangular face of a down-pointing pyramid in comparison with equation (1) of Patrick *et al.* [1] for an inclined rectangular surface, may be explained by the fact that the triangular surface is fed by a fresh electrolyte, not only at the lower edge of the surface, as for a rectangular face, but all along the inclined edges of the triangle. This must inevitably lead to a higher mean mass transfer coefficient.

Results for the mass transfer to the horizontal triangular upward facing surface are shown in Fig. 5 as a plot of Sherwood number against Rayleigh number, with the height of the triangular horizontal base ( $H_h$ ) as characteristic dimension. The least square analysis gives the correlation

$$Sh_{H_h} = 0.203(Ra_{H_h})^{0.323}. \quad (13)$$

Forcing a slope of 1/3 as reported in the literature for turbulent flow on upward facing horizontal planes [4–7, 20] gives the relation:

$$Sh_{H_h} = 0.176(Ra_{H_h})^{0.33} \quad (14)$$

for  $Ra_{H_h}$  in the range from  $5 \times 10^7$  to  $2.2 \times 10^{10}$ . This equation is plotted as the broken line in Fig. 5. This gives very good agreement with the correlation for upward facing surfaces given by Patrick *et al.* [21].

### 3.3. Mass transfer at combinations of surfaces

Mass transfer coefficients for all the inclined triangular surfaces for different pyramid lengths of pyramids 11–15 are shown in Fig. 6 for four different  $CuSO_4$  concentrations. The mass transfer correlation

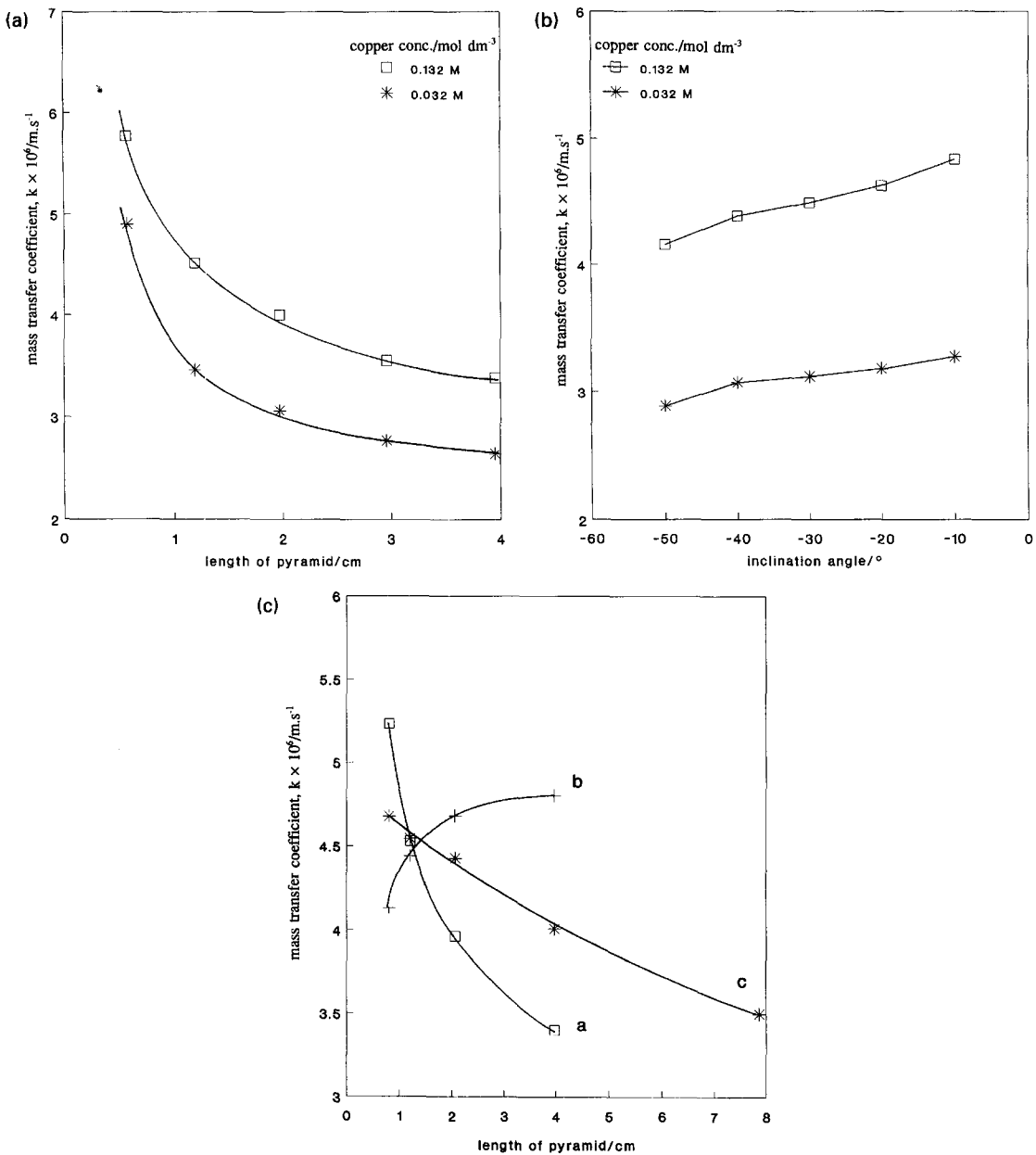


Fig. 3. (a) The effect of length on mass transfer coefficient of a single inclined surface of a down-pointing pyramid of constant inclination angle (pyramids 1-5). (b) The effect of inclination angle on mass transfer coefficient of a single inclined surface of a down-pointing pyramid of constant length (pyramids 6-10). (c) Simultaneous effect of length and inclination angle on mass transfer coefficient at a single inclined surface of a down-pointing pyramid,  $c = 0.132 \text{ M}$ , □ pyramids 1-5 (constant angle), + pyramids 6-10 (constant length), \* pyramids 11-15.

for all the inclined surfaces simultaneously active is shown in Fig. 7. Forcing a slope of 1/4 gives the relationship

$$Sh_L = 0.714(Ra_{L,\theta})^{0.25} \quad (15)$$

for the same  $Ra_{L,\theta}$  range as equation (12). The coefficient in equation (15) is lower than that in equation (12), since the mass transfer rates at the single inclined surfaces are not additive because of interactions at the pyramid edges. However, mass transfer

is still higher than for inclined rectangular faces [1, 2, 15, 20].

Mass transfer for the separate surfaces of pyramids 11-15 and for the surfaces in combination are plotted in Fig. 8 for a single concentration of copper sulphate (0.132 M). This clearly shows the superior mass transfer performance of the up-facing horizontal surface and the fact that a single triangular inclined surface gives higher mass transfer than the combined inclined surfaces.

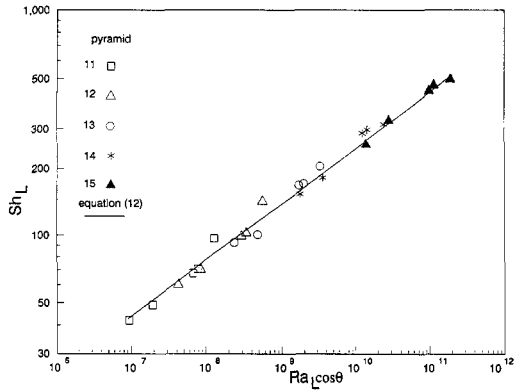


Fig. 4. Mass transfer correlation for single inclined triangular surfaces.

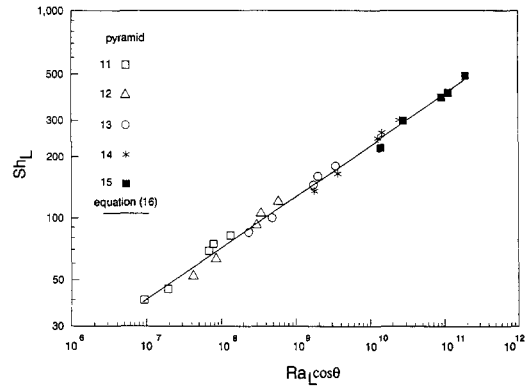


Fig. 7. Mass transfer correlation for all inclined faces simultaneously active.

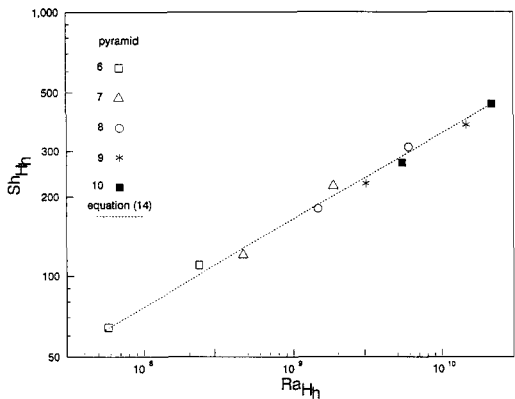


Fig. 5. Mass transfer correlation for upward-facing horizontal triangular surfaces.

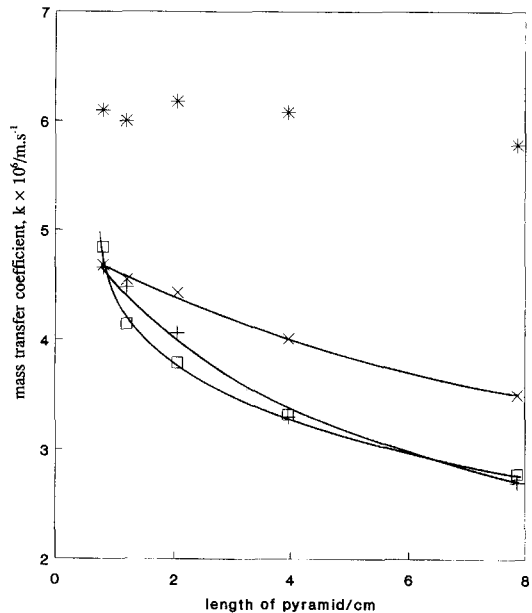


Fig. 8. The effect of length on mass transfer coefficient for different surfaces for a single concentration of copper sulphate (constant pyramid base). Pyramid surfaces considered,  $\times$  single inclined triangular surface,  $+$  combination of all inclined triangular surfaces,  $*$  upward-facing horizontal surface,  $\square$  total surface.

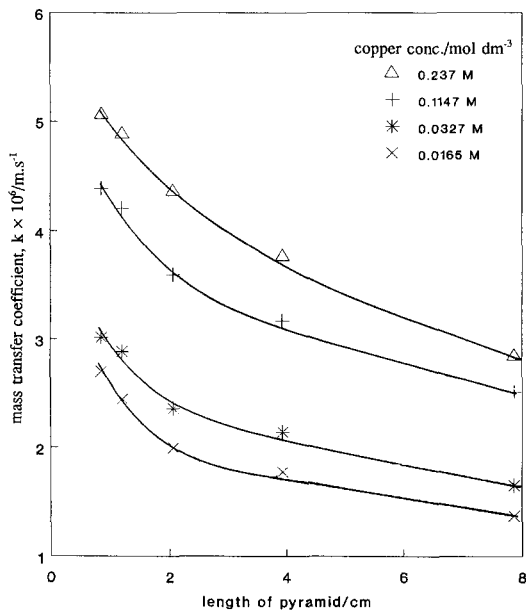


Fig. 6. The effect of length (and inclination angle) on mass transfer coefficient for all inclined surfaces simultaneously active (constant pyramid base).

The effect of pyramid length,  $L$  (and inclination angle), on the mass transfer coefficient for the entire pyramids 11–15 is shown in Fig. 9 for four different  $\text{CuSO}_4$  concentrations.

3.4. Overall data correlation

3.4.1. Approach using Weber characteristic dimension. The total mass transfer results from pyramids 11–15 are plotted using the characteristic length defined by Weber *et al.* [8] in Fig. 10. The Weber correlation (equation (5)) is also shown. It is seen that the data from all the present pyramids lie above equation (5). This may be explained by several facts :

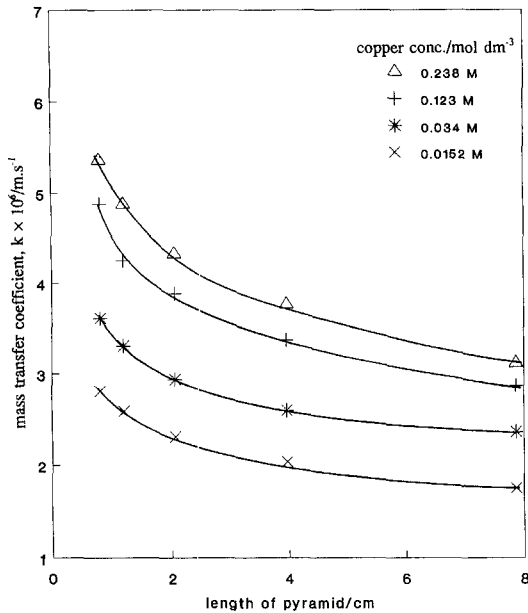


Fig. 9. The effect of length on total mass transfer coefficient for downpointing pyramid (constant pyramid base).

- (i) the term expressing the influence of inclination angle is not present in the Weber correlation;
- (ii) Weber recommended equation (5) for objects with sphericity  $\Psi > 0.6$  and two of the present pyramids (11 and 15) have sphericity values outside this limit;
- (iii) the down-pointing pyramids have no down-facing horizontal surface as do other three dimensional objects (cuboids, vertical cylinders).

Worthington *et al.* [10] and the present authors [11] also observed discrepancy with the Weber approach when correlating natural convective mass transfer data to cuboids [10] and vertical cylinders with active ends [11]. Nevertheless this probably presents the best possible correlation based on a single characteristic

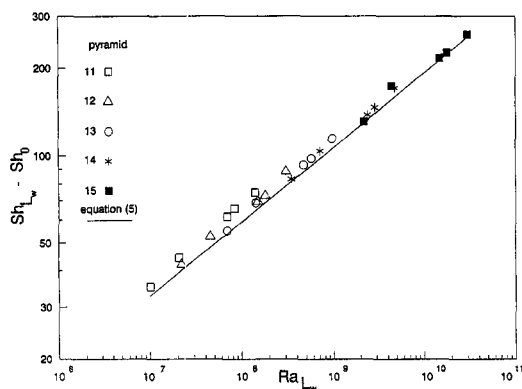


Fig. 10. Correlation of total pyramidal mass transfer data using the Weber *et al.* [8] characteristic dimension.

length and a least squares fit through data yields the relation:

$$Sh_{L_w} - Sh_0 = 0.673(Ra_{L_w})^{0.247} \quad (16)$$

for  $Ra_{L_w}$  in the range  $1 \times 10^7$  to  $3 \times 10^{10}$ .

3.4.2. *Summation approach to correlation for entire down-pointing pyramids.* By summing the mass transfer rates from correlations for the separate sides the total mass transfer performance can be predicted. The advantage of this method is discussed in refs. [10, 11]. In the present approach the correlation for all the inclined surfaces was taken as equation (15). For the upward facing horizontal surfaces the correlation was taken as equation (14), which is in excellent agreement with the correlation of Patrick and Wragg [21]. The mass transfer rates for separate surfaces were correlated using length of pyramid ( $L$ ) and height of horizontal base of pyramid ( $H_b$ ) as characteristic lengths. The resultant predicted natural convection mass transfer rate for down-pointing pyramids becomes

$$Sh_L - Sh_0 = \frac{[4.284L(\cos \theta)^{0.25} + 0.3048bRa_L^{1/12}]}{6L + b\sqrt{3}} Ra_L^{0.25} \quad (17)$$

in the region  $9 \times 10^6 \leq Ra_L \leq 2 \times 10^{11}$ .

Introducing the relationship

$$\cos \theta = \frac{\sqrt{L^2 - \frac{1}{12}b^2}}{L} \quad (18)$$

to equation (17) yields

$$Sh_L - Sh_0 = \frac{[4.284L^{3/4}(L^2 - \frac{1}{12}b^2)^{1/8} + 0.3048bRa_L^{1/12}]}{6L + b\sqrt{3}} Ra_L^{0.25} \quad (19)$$

where  $L$  and  $b$  are the inclined surface pyramid length and the base of the horizontal surface of the pyramid, respectively, and  $Ra_L$  is a Rayleigh number based on the length of the inclined surface of the pyramid.

3.4.3. *Summation approach with interference.* The behaviour predicted by equation (19) was compared with the mass transfer data for pyramids 11–15. It was found in every case that the predicted rate was higher than the actual data, but that the shape and gradient of the prediction were well matched. The flow of the fluid up the inclined surfaces of the pyramid means that the upward facing horizontal surface is exposed to a solution which has already been depleted of copper ions. Thus, the overall mass transfer for a pyramid is lower than that for the equivalent summed separate surfaces (see Fig 8). A multiplying factor,  $f$  (an interference factor), may be introduced to equation (19) to represent the lower rate of mass transfer at the upward facing horizontal surface. This equation now

Table 2. Dependence of interference factor,  $f$ , on pyramid geometry

| Pyramid | 11   | 12   | 13   | 14   | 15   |
|---------|------|------|------|------|------|
| $f$     | 0.91 | 0.76 | 0.67 | 0.63 | 0.58 |

becomes

$$Sh_L - Sh_0 = \frac{[4.284L^{3/4}(L^2 - \frac{1}{12}b^2)^{1/8} + f(0.3048bRa_L^{1/12})]}{6L + b\sqrt{3}} \times Ra_L^{0.25} \quad (20)$$

for turbulent flow.

Values of  $f$  were obtained from equation (20) and calculated for each pyramid. These are tabulated in Table 2.  $f$  varies between 0.58 for the tallest pyramid and 0.91 for the smallest pyramid.  $Sh_L - Sh_0$  has been plotted to show the data from pyramids 11–15 against  $\phi(L, b, Ra_L)$ .  $Ra_L$  in Fig. 11.  $\phi(L, b, Ra_L)$  is given by  $\phi(L, b, Ra_L) =$

$$\left[ \frac{4.284^{3/4}(L^2 - \frac{1}{12}b^2)^{1/8} + f(0.3048bRa_L^{1/12})}{6L + b\sqrt{3}} \right]^4 \quad (21)$$

for turbulent flow.

It can be seen that all the data fit the line representing equation (20) very well. All the points lie within a deviation of 3–4% from the line and the fit is much better than that for the Weber correlation. Figure 12 shows the dependence of  $f$  on the pyramidal aspect ratio ( $L/b$ ). The plot shows that for low values of  $L/b$  (from 0.35 to 0.8) the interference factor decreases strongly and for higher values of  $L/b$  (1.5 and more) the decrease is much more gradual.

As with work reported in refs. [10] and [11], the separate sides summation approach incorporating an interference factor has proved highly successful in correlating mass (heat) transfer data for natural con-

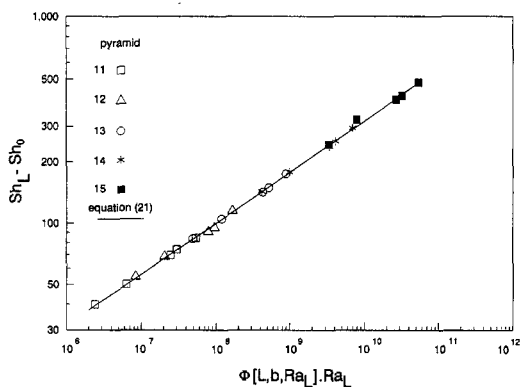


Fig. 11. Overall correlation of entire pyramid data in terms of equation (20).

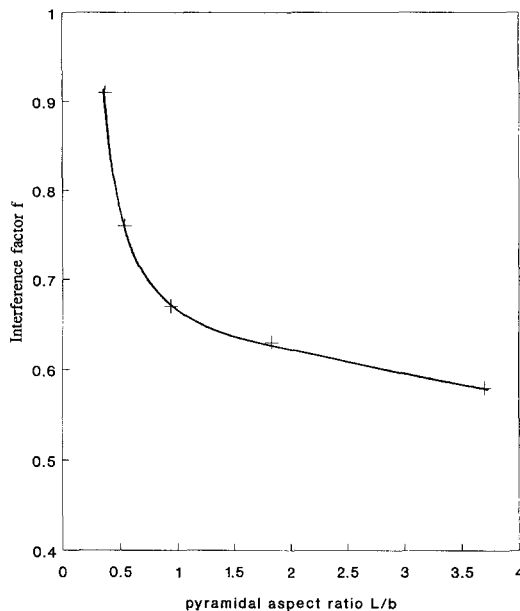


Fig. 12. Plot showing variation of interference factor,  $f$ , with pyramidal aspect ratio  $L/b$ .

vection at a three-dimensional solid, and may be recommended for design calculation purposes.

## REFERENCES

1. M. A. Patrick, A. A. Wrapp and D. M. Pargeter, Mass transfer by free convection during electrolysis at inclined electrodes, *Can. J. Chem. Engng* **55**, 432–438 (1977).
2. J. R. Lloyd, E. M. Sparrow and E. R. G. Eckert, Laminar transition and turbulent natural convection adjacent to inclined and vertical surfaces, *Int. J. Heat Mass Transfer* **15**, 457–473 (1972).
3. M. G. Fouad and A. M. Ahmed, Mass transfer by free convection at inclined electrodes, *Electrochim. Acta* **14**, 651–666 (1969).
4. E. S. Fenech and C. W. Tobias, Mass transfer by free convection at horizontal electrodes, *Electrochim. Acta* **2**, 311–321 (1960).
5. A. A. Wrapp, Free convection mass transfer at horizontal electrodes, *Electrochim. Acta* **13**, 2159–2165 (1968).
6. A. A. Wrapp and R. P. Loomba, Free convection flow patterns at horizontal surfaces with ionic mass transfer, *Int. J. Heat Mass Transfer* **13**, 439–442 (1970).
7. J. R. Lloyd and W. R. Moran, Natural convection adjacent to horizontal surface of various planforms, *J. Heat Transfer* **96**, 443–447 (1974).
8. M. E. Weber, P. Austraukas and S. Petsalis, Natural convection mass transfer to nonspherical objects at high Rayleigh number, *Can. J. Chem. Engng* **62**, 68–72 (1984).
9. G. H. Sedahmed and I. Nirdosh, Free convection mass transfer at horizontal cylinders with active ends, *Int. Commun. Heat Mass Transfer* **17**, 355–364 (1990).
10. D. R. E. Worthington, M. A. Patrick and A. A. Wrapp, Effect of shape on natural convection heat and mass transfer at horizontally oriented cuboids, *Chem. Engng Res. Des.* **65**, 131–138 (1987).
11. J. Krysa and A. A. Wrapp, Free convective mass transfer at vertical cylindrical electrodes of varying aspect ratio, *J. Appl. Electrochem.* **22**, 429–436 (1992).
12. R. J. Goldstein, E. M. Sparrow and D. C. Jones, Natural convection mass transfer adjacent to horizontal plates, *Int. J. Heat Mass Transfer* **16**, 1025–1034 (1973).



13. M. A. Patrick and A. A. Wragg, Modelling of free convection in heat transfer using electrochemical mass transfer techniques, *J. Chem. Engrg Symp. Series* **94**, 45–55 (1985).
14. A. F. J. Smith and A. A. Wragg, An electrochemical study of mass transfer in free convection at vertical arrays of horizontal cylinders, *J. Appl. Electrochem.* **4**, 219–228 (1974).
15. M. A. Patrick and A. A. Wragg, Steady and transient natural convection at inclined planes and cones, *Phys.-chem. Hydrodyn.* **5**, 299–306 (1984).
16. M. Eisenberg, C. W. Tobias and C. R. Wilke, Selected properties of ternary electrolytes employed in ionic mass transfer studies, *J. Electrochem. Soc.* **103**, 413–416 (1956).
17. C. R. Wilke, M. Eisenberg and C. W. Tobias, Correlation of limiting currents under free convection conditions, *J. Electrochem. Soc.* **100**, 513–517 (1953).
18. N. Ibl and O. Dossenbach, *Comprehensive Treatise of Electrochemistry*, Vol. 6 (Edited by E. Yeager, J. O'M. Bockris, B. E. Conway and S. Sarangapani), pp. 192–198. Plenum Press, New York (1983).
19. R. Clift, J. R. Grace and M. E. Weber, *Bubbles, Drops and Particles*, pp. 88–91. Academic Press, New York (1978).
20. T. Fujii and H. Imura, Natural convection heat transfer from a plate with arbitrary inclination, *Int. J. Heat Mass Transfer* **15**, 755–756 (1972).
21. M. A. Patrick and A. A. Wragg, Optical and electrochemical studies of transient free convective mass transfer at horizontal surfaces, *Int. J. Heat Mass Transfer* **18**, 1397–1407 (1975).